© 2022. Published by The Company of Biologists Ltd | Journal of Experimental Biology (2022) 225, jeb243328. doi:10.1242/jeb.243328

RESEARCH ARTICLE

Escaping from multiple visual threats: modulation of escape responses in Pacific staghorn sculpin (*Leptocottus armatus*)

Hibiki Kimura[1,*], Tilo Pfalzgraff[2], Marie Levet[3], Yuuki Kawabata[1], John F. Steffensen[4], Jacob L. Johansen[5] and Paolo Domenici[6,7]

ABSTRACT

Fish perform rapid escape responses to avoid sudden predatory attacks. During escape responses, fish bend their bodies into a C-shape and quickly turn away from the predator and accelerate. The escape trajectory is determined by the initial turn (stage 1) and a contralateral bend (stage 2). Previous studies have used a single threat or model predator as a stimulus. In nature, however, multiple predators may attack from different directions simultaneously or in close succession. It is unknown whether fish are able to change the course of their escape response when startled by multiple stimuli at various time intervals. Pacific staghorn sculpin (*Leptocottus armatus*) were startled with a left and right visual stimulus in close succession. By varying the timing of the second stimulus, we were able to determine when and how a second stimulus could affect the escape response direction. Four treatments were used: a single visual stimulus (control); or two stimuli coming from opposite sides separated by a 0 ms (simultaneous treatment), 33 ms or 83 ms time interval. The 33 ms and 83 ms time intervals were chosen to occur either side of a predicted 60 ms visual escape latency (i.e. during stage 1). The 0 ms and 33 ms treatments influenced both the escape trajectory and the stage 1 turning angle, compared with a single stimulation, whereas the 83 ms treatment had no effect on the escape trajectory. We conclude that Pacific staghorn sculpin can modulate their escape trajectory only between stimulation and the onset of the response, but the escape trajectory cannot be modulated after the body motion has started.

KEY WORDS: C-start, Escape trajectory, Fast start, Sensory feedback, Looming stimuli, Fish escape response, Predation, Visual stimuli

INTRODUCTION

Fish avoid predators by performing sudden accelerations, i.e. fast start escape responses (Domenici and Blake, 1997). The kinematics and neural control of escape responses have been widely investigated (Domenici and Blake, 1993; Domenici and Hale, 2019; Eaton et al., 2001; Stewart et al., 2014). Fish escape responses typically consist of C- or S-starts, based on the shape of the fish at the end of the first contraction (Domenici and Hale, 2019). In C-starts, fish bend their bodies into a C-shape during the initial muscle contraction (stage 1), usually away from the threat, while a subsequent return flip of the tail (when present; Domenici and Hale, 2019) can produce further acceleration (stage 2) (Fleuren et al., 2018).

Fish can be startled using a variety of stimuli, from mechano-acoustic to tactile and visual stimuli (Domenici and Hale, 2019). The shortest latencies are typically associated with the stimulation of the mechano-acoustic sensory system, leading to the activation of the Mauthner cells (M-cells) (Korn and Faber, 2005), whereas visual stimuli tend to show longer latencies because of the longer neural pathway (Mirjany and Faber, 2011) from the optic nerve to the M-cell via the optic tectum (Temizer et al., 2015). M-cell ablation was shown to delay the escape response and to decrease survival in predator–prey encounters (Hecker et al., 2020).

Most previous studies on fish escape responses have focused on a single threat such as a model or a real predator approaching, resulting in an escape response directed away from the threat (Domenici and Blake, 1993; Stewart et al., 2013, 2014; Walker et al., 2005). However, in nature, multiple predators may attack prey from two or more directions simultaneously or in close succession (Amo et al., 2004; Bshary et al., 2006; Stander, 1992; Steinegger et al., 2018). Multiple co-occurring threats are known to affect the prey's escape directions; for example, lizards escape ∼180 deg away from single predators but perpendicular to the predators when attacked simultaneously from two opposite directions (Cooper et al., 2007).

Previous work has investigated the possibility that a modification of the escape trajectory can occur after initial stimulation. Importantly, inhibition of the mechanosensory input occurs during stage 1 in both C- and S-starts (Russell, 1976), leading Eaton et al. (1981) and Eaton and Emberley (1991) to suggest that the neural command underlying the escape response is ballistic once the movement has begun (i.e. without further sensory information to compute its trajectory). Indeed, Eaton et al. (1988) found that the stage 2 command of the goldfish is preprogrammed and not dependent on sensory feedback; however, it remains unknown whether sensory feedback can occur before or after the initiation of stage 1.

Some taxa are able to modulate escape responses to multiple successive attacks. Certain crickets, for instance, were found to use two escape modes (i.e. running and jumping) with different degrees of flexibility: when crickets escaped from an initial predator attack by running, they were able to modulate their trajectory in response to a second attack; however, this was not that case for crickets that escaped from the initial attack by jumping (i.e. a ballistic response) (Sato et al., 2019). Recent work has shown that larval zebrafish may be able to integrate sensory information from multiple threats during delayed escape responses through a cluster of 38 prepontine neurons

[1]Graduate School of Fisheries and Environmental Sciences, Nagasaki University, 1-14 Bunkyo-machi, Nagasaki 852-8521, Japan. [2]Technical University of Denmark, DTU AQUA, Section for Aquaculture, The North Sea Research Centre, 9850 Hirtshals, Denmark. [3]Département de Sciences Biologiques, Université de Montréal, Campus MIL, 1375 Avenue Thérèse-Lavoie-Roux, Montréal, QC, Canada, H2V 0B3. [4]Marine Biological Section, Department of Biology, University of Copenhagen, Strandpromenaden 5, DK-3000 Helsingør, Denmark. [5]Hawaii Institute of Marine Biology, University of Hawaii at Manoa, 46-007 Lilipuna Rd, Kaneohe, HI 96744, USA. [6]CNR-IBF, Institute of Biophysics, 56124 Pisa, Italy. [7]CNR-IAS, Institute for the Study of Anthropic Impacts and Sustainability in the Marine Environment, 09072 Torregrande (Oristano), Italy.

*Author for correspondence (h.kimura787@gmail.com)

H.K., 0000-0003-3710-2564; T.P., 0000-0001-8059-6534

Received 12 August 2021; Accepted 5 April 2022

Journal of Experimental Biology (2022) 225, jeb243328. doi:10.1242/jeb.243328

that are not part of the fast escape neural pathway (Marquart et al., 2019). This finding suggests that during the initial escape latency (i.e. before the onset of stage 1 contraction), fish may have the potential to integrate sensory information from multiple threats. Additionally, Domenici and Blake (1993) suggested that sensory feedback may occur after the onset of stage 1, resulting in a correction of escape trajectories during stage 2. Hence, the extent of stage 2 may, at least in part, be controlled by a feedback system (Domenici and Blake, 1993).

Here, we investigated the possibility that escape kinematics may vary depending on the time difference between the two visual threat stimuli coming from opposite sides. Visual looming stimuli are known to trigger an escape response once a given threshold (that depends on the size and speed of the approaching object) is reached (Cade et al., 2020; Hein et al., 2018). We hypothesized that if the escape response is fully ballistic from the time of the first stimulation, the escape kinematics will not be modified by a second stimulus delivered at any time interval >0 ms after the first one. If, in contrast, the escape kinematics is modified by a second stimulus, this indicates that sensory feedback is possible during that time interval.

MATERIALS AND METHODS

Ethics statement

All animal care and experimental protocols followed the guidelines of the Institutional Animal Care and Use Committee at the University of Washington, Seattle, WA, USA (Protocol No. 4238-03).

Model species and housing conditions

Pacific staghorn sculpin [*Leptocottus armatus* Girard 1854, mean±s.d. total length (TL) 13.9±1.71 cm; n=71] were captured by beach seining at Jackson Beach, south of San Juan Island, WA, USA (48°31′11″N, 123°0′45″W) in July 2019. The fish were maintained in two acrylic tanks (87 cm length×57 cm width×14 cm depth) with flow-through seawater under a 14 h:10 h light:dark photoperiod, at 12.5±0.5°C. They were acclimatized for ≥24 h and fed shrimp pieces every second day. At the end of the experiment, they were released at Jackson Beach.

Experimental setup

Experiments were conducted at Friday Harbor Laboratories, University of Washington, in an acrylic fish tank (125.5 cm length×57 cm width×35 cm depth; Fig. 1A) filled with seawater at 12.5±0.5°C. White plastic panels were placed on the tank walls and bottom. A white plastic panel with grid lines (48 cm×34 cm) was placed at the bottom center of the tank. Two 300 W halogen lamps were set above the tank to illuminate it. A high-speed camera (640×360 pixels, 240 frames s^{-1}; Stylus TG-870, Olympus Corp., Tokyo, Japan) was positioned 110 cm above the tank and recorded the escape response.

Two looming stimuli were used. Each stimulus was played on a separate screen (1600×1200 pixels, 60 Hz; Dell 2000FP, Dell Inc., Round Rock, TX, USA) placed centrally on opposing sides of the experimental tank (Fig. 1A). Each stimulus simulated a black disk (24 cm diameter) approaching from 200 cm distance at a constant velocity of 1 m s^{-1}. The movie of the looming stimulus

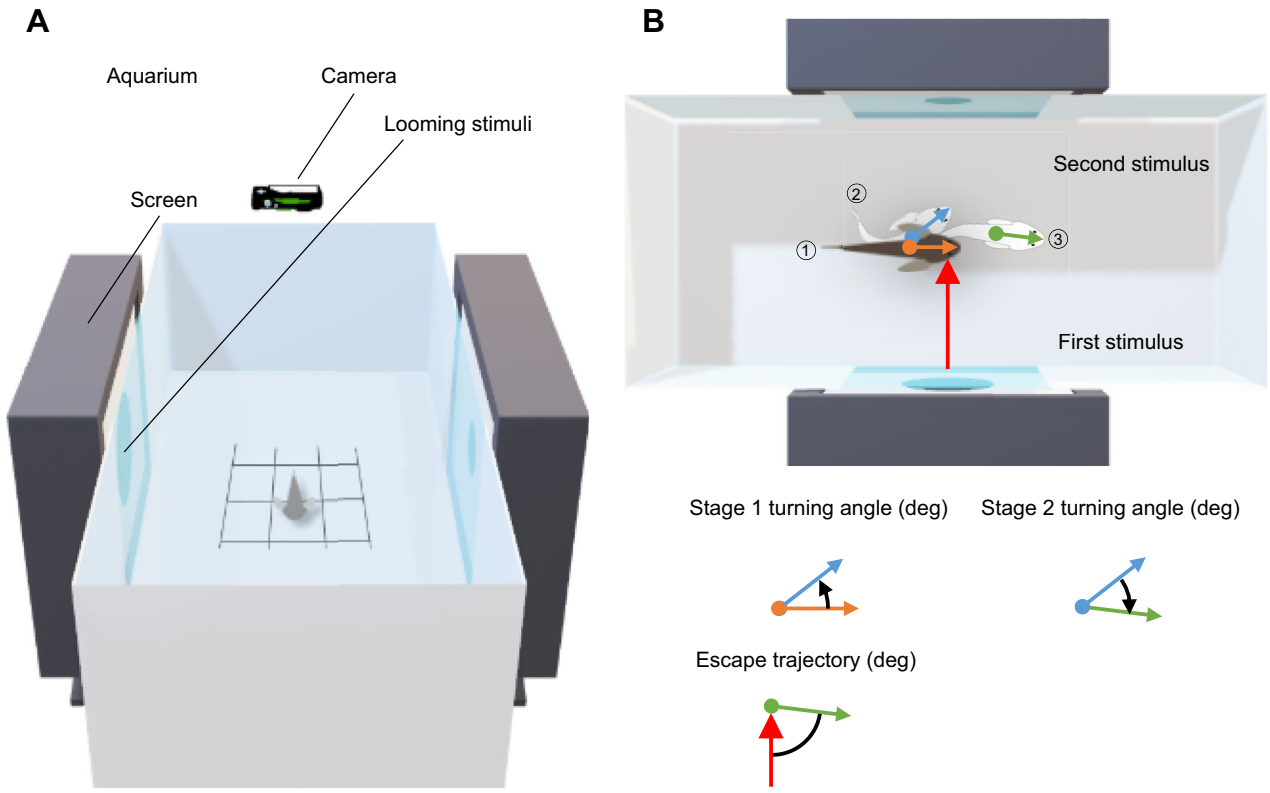

Fig. 1. Experimental setup and measurements. (A) Schematic representation of the setup. Two screens were used to stimulate fish from the left and right sides with looming stimuli. Fish were always oriented parallel to the long axis of the aquarium (90 deg initial orientation). (B) Definitions of stage 1 and 2 turning angles and escape trajectory. Upper diagram shows fish just before onset of the escape response (1), at end of stage 1 (2) and the end of stage 2 (3). Lower diagrams show variable definitions. Orange, blue and green vectors represent fish directions just before onset of the escape response, at the end of stage 1, and at the end of stage 2, respectively. The red arrow represents the first stimulus direction. Each filled circle on an arrow represents fish center of mass (CoM).

Journal of Experimental Biology (2022) 225, jeb243328. doi:10.1242/jeb.243328

(1600×1200 pixels; 60 frames s^{-1}) was created with R v.3.6.1 (http://www.R-project.org/) using the package *loomeR* v.0.3.0 (doi:10.5281/zenodo.3279092). To control the delay of one movie from the other, two movies were stitched together horizontally using Shotcut Video Editor v.19.07 (Meltytech LLC, Walnut Creek, CA, USA) and each side of the movie was played on a separate screen by the extended dual display mode. For the 0 ms treatment, two identical movies were stitched together and played simultaneously. For the 33 ms treatment, one of the two movies (second stimulus) was played with a delay of two frames (~33 ms) relative to the first stimulus. For the 83 ms treatment, the second stimulus was played with a delay of five frames (~83 ms). For the control, only a single looming stimulus was played. The side of the first stimulus was randomized. The times for the delayed stimuli (33 ms and 83 ms) were selected based on the estimated visual escape latency of *L. armatus* (60 ms; Paglianti and Domenici, 2006). Hence, the stimulus delayed by 33 ms was assumed to be within the escape latency of *L. armatus* (defined as the time interval between the stimulus-reaching threshold and the fish response, corresponding to neurosensory processing prior to the visible response; Paglianti and Domenici, 2006) (Fig. 2), whereas the stimulus delayed by 83 ms was assumed to occur during stage 1 (Fig. 2).

Experimental procedure

Each fish was transferred to the experimental tank and placed in an opaque PVC shelter (15.5 cm diameter) where it was allowed to acclimatize for 15 min. A square panel under the tank bottom was used as a placement reference, ensuring that all fish were placed in the center of the tank at a distance >1.5 body lengths away from the walls to avoid any interference with their escape trajectory (Eaton and Emberley, 1991). The fish were placed perpendicular to the stimuli by carefully rotating the PVC shelter [86.76±10.93 deg; n=66].

After acclimatization to the experimental tank, the shelter was removed and fish were left undisturbed for an additional 2 min, after which they were startled. Each fish was exposed to each of the four treatments (in random order) only once. The side of the first looming stimulus was randomly selected. Between stimuli, the fish were returned to the PVC shelter to avoid stimulation prior to each treatment. Fish were allowed at least 2 min to recover from the previous stimulation before the next trial continued. If fish moved before the stimulation, they were returned to the PVC shelter and were acclimatized for an additional 2 min. If the ventilation rate was higher than at rest (i.e. a sign of an elevated stress level) by our visual observation, extra time was allocated until the ventilation rate decreased before the next stimulus was played.

Data and statistical analysis

The 240 frames s^{-1} video of the escape response was analyzed frame by frame with Logger Pro v.3.15 (Vernier Software & Technology, Beaverton, OR, USA). The only responses used were those in which the fish reacted to the stimuli and initiated an escape response to the first stimulus (total 66 responses: 0 ms treatment, 18 responses; 33 ms treatment, 13 responses; 83 ms treatment, 16 responses; control, 19 responses). The fish snout and center of mass (CoM; 35% of total body length; Paglianti and Domenici, 2006) were digitalized in each frame.

A total of six biomechanical and five time–distance variables were then calculated (Dadda et al., 2010; Domenici and Ruxton, 2015). The escape trajectory (deg) was calculated as the angle between the direction of the line passing through the CoM and the snout at the end of stage 2 and the virtual movement direction of the first stimulus (Fig. 1A). The stage 1 turning angle (deg) was calculated as the angle between the line passing through the CoM and the snout at the onset of stage 1 and that at the onset of stage 2 (Fig. 1B). Stage 1 was taken as the time interval between the onset of stage 1 and the onset of stage 2 (stage 1 turning duration; ms). The stage 1 turning rate (deg s^{-1}) was calculated by dividing the stage 1 turning angle by the stage 1 turning duration. The stage 2 turning angle (deg) was calculated as the angle between the line passing through the CoM and the snout at the onset of stage 2 and that at the

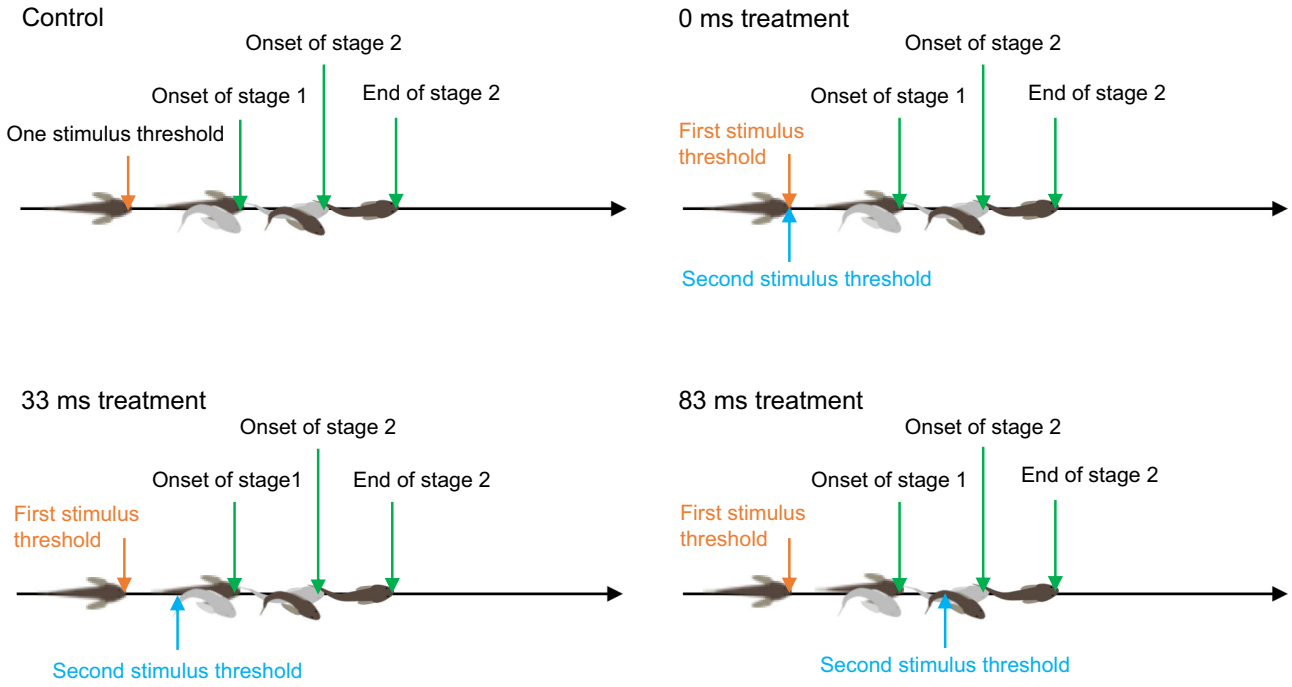

Fig. 2. Concepts of the four treatments. Diagrams show transitions of stimuli and fish responses for each treatment. Thresholds represent the onset of neural processing of the escape response.

Journal of Experimental Biology (2022) 225, jeb243328. doi:10.1242/jeb.243328

end of stage 2 (Fig. 1B). Stage 2 was taken as the time from the onset to the end of stage 2 (stage 2 turning duration; ms). The stage 2 turning rate (deg s^{-1}) was calculated by dividing the stage 2 turning angle by the stage 2 turning duration. The apparent looming threshold (ALT; rad s^{-1}) triggering the escape response was calculated using Eqn 1 (Dill, 1974):

$$\frac{d\alpha}{dt} = \frac{4VS}{4D^2 + S^2}, \quad (1)$$

where α is the angular size (deg) of the black disk, D is the virtual distance between the nearest fish eye and the virtual object (cm), S is the size of the virtual object (24 cm virtual diameter) and V is the apparent speed of the approaching object (100 cm s^{-1}).

The time–distance variables maximum acceleration (m s^{-2}), maximum speed (cm s^{-1}) and cumulative distance (cm) were measured based on the CoM displacement. These variables were evaluated between the onset of stage 1 and the end of stage 2. Maximum acceleration and maximum speed were calculated by first- and second-order differentiation, respectively, of the cumulative distance for the time series. A Lanczos five-point quadratic moving regression method (Lanczos, 1956) was applied to calculate these last two values.

Each variable in each treatment was fitted with one- to nine-component Gaussian mixture distributions (GMD) with equal and unequal variance (total 17 GMD models) with an expectation-maximization (EM) algorithm. The most parsimonious probability distribution on each variable was chosen based on the lowest Akaike information criterion (AIC). Then, in all variables, a dominant normal distribution of GMD of each treatment was compared with that of the control with Dunnett-corrected 95% confidence intervals (Dunnett, 1964). As a *post hoc* test, the three treatments (0 ms, 33 ms and 83 ms) were compared with each other using an information-theoretic (I-T) approach, which can be used for multiple comparisons between treatments, and has several advantages over conventional methods such as Tukey HSD (Burnham et al., 2011; Dayton, 1998; Sugiura, 1978). The I-T approach allows comparison of models with differing distributions (e.g. GMD) (Domenici et al., 2008) and nesting/non-nesting (Halsey, 2019; Richards et al., 2011), and is robust to the fact that the distribution of some variables in our data was not unimodal (based on a visual assessment; Fig. S1). Our three treatments (0 ms, 33 ms and 83 ms) allowed for 5 combinations of comparisons by categorizing each group as the same (=) or different (≠) (e.g. 0 ms=33 ms≠83 ms; see Fig. S2 for combination details). AIC was calculated with the following equation:

$$\mathrm{AIC} = -2\log L + 2k, \quad (2)$$

where k is the number of parameters and log$L$ is the model log-likelihood. For example, parameters of normal distribution are a mean and variance. Thus, k is 2. In the case of two-component GMD with unequal variance, this GMD has two independent normal distributions, i.e. it has two means and two variances. To adjust the total probability to 100%, it also has a mixing probability. Thus, k is 5. In general, k was calculated with the following equation:

$$k = k_{\mathrm{gaussian}} N_{\mathrm{group}} + (N_{\mathrm{group}} - 1), \quad (3)$$

where k_{gaussian} is the number of parameters of the GMD (see Table 1) and N_{group} is the number of groups in the model (see Fig. S2). log$L$ was calculated with the following equation:

$$\log L = \sum \log L_{\mathrm{group}}, \quad (4)$$

where logL_{group} is the log-likelihood of each pooled group. The data categorized in the same group were pooled to estimate logL_{group}. For example, in a combination where '0 ms=33 ms≠83 ms', the 0 ms treatment is not different from the 33 ms treatment, but is different from the 83 ms treatment, and the 33 ms treatment is different from the 83 ms treatment. In that scenario, the data of the 0 ms and 33 ms treatments were pooled to estimate the first logL_{group}, and the second logL_{group} of the 83 ms treatment data was estimated independently. Then, the two logL_{group} were summed to calculate the AIC. In an extreme case where '0 ms=33 ms=83 ms', data from all three treatments were pooled to estimate the logL_{group} and AIC, whereas if '0 ms≠33 ms≠83 ms', the data of these three treatments were separately analyzed to estimate each logL_{group}, and the logL_{group} of the three treatments were summed up to calculate the AIC. The most parsimonious model on each of the 11 variables was then chosen based on the lowest AIC. The AIC difference (ΔAIC) was calculated between the best model and all others. Potential models were those with ΔAIC<2 (Sugiura, 1978).

All estimations of the GMDs, comparisons with a control with Dunnett-corrected 95% confidence intervals, and the analysis of the I-T approach to find differences among treatments were performed in R v. 3.6.1 (http://www.R-project.org/) with the *Mclust* v.5.4.5 package (Scrucca et al., 2016). Because some complex models of each variable could not be calculated with the *Mclust* package as a consequence of a singularity in the covariance matrix (Scrucca et al., 2016), the analysis of the I-T approach was performed only on models that could be calculated. Although escape trajectories are circular variables which potentially span 360 deg (Domenici et al., 2011), most escape trajectories were distributed through a limited arc and the uniformity of the escape trajectories was not supported by Watson's goodness of fit test for a circular uniform distribution (U^2 test; 0 ms: U^2=0.86, P<0.01; 33 ms: U^2=0.54, P<0.01; 83 ms: U^2=0.60, P<0.01; control: U^2=0.79, P<0.01) and escape trajectories were not distributed around 360 deg (Fig. 3A). Therefore, the distributions and the difference between treatments

Table 1. Models of Gaussian mixture distributions

No.	G	V_{gaussian}	k_{gaussian}
1	1	X	2
2	2	E	4
3	3	E	6
4	4	E	8
5	5	E	10
6	6	E	12
7	7	E	14
8	8	E	16
9	9	E	18
10	2	V	5
11	3	V	8
12	4	V	11
13	5	V	14
14	6	V	17
15	7	V	20
16	8	V	23
17	9	V	26

G, number of components of Gaussian mixture distribution; V_{gaussian}, model of variance of Gaussian mixture distribution; X, normal Gaussian distribution; E, Gaussian mixture distributions with equal variance; V, Gaussian mixture distributions with unequal variance; k_{gaussian}, number of parameters of Gaussian mixture distribution.

Journal of Experimental Biology (2022) 225, jeb243328. doi:10.1242/jeb.243328

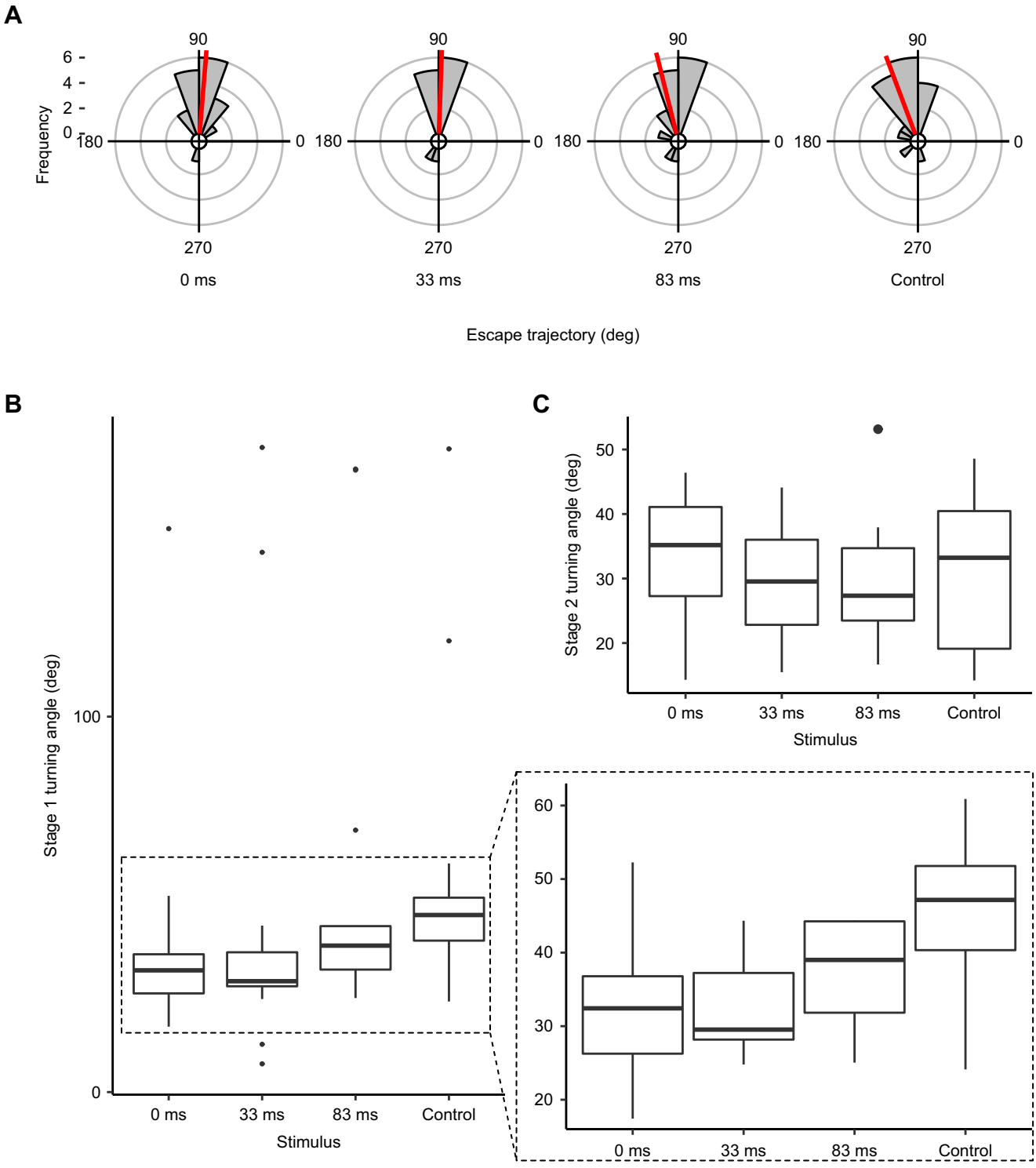

Fig. 3. Escape trajectories. (A) Circular histogram of escape trajectories. Red lines show the circular mean value for each treatment. The bin intervals are 20 deg. The initial orientation of fish is 90 deg. (B,C) Boxplots of stage 1 turning angles excluded outliers (B) and stage 2 turning angles (C). Boxes represent median, and lower and upper quartiles. Ends of vertical lines are minima and maxima. Filled circles are values >1.5× the upper quartile (outliers). Inset in B shows the stage 1 turning angles in the range 16–63 deg.

were analyzed using linear statistics (estimation of the GMD and the analysis of the I-T approach) as suggested by Batschelet (1981). Calculations of variables and statistical analyses were performed in R v. 3.6.1 with the *circular* v.0.4-93 package (https://r-forge.r-project.org/projects/circular/).

RESULTS

A summary of the statistical analyses on the kinematic variables is shown in Tables 2 and 3 and Tables S1 and S2. The escape trajectories, stage 1 turning angle, stage 1 turning duration and stage 1 turning rate of the 0 ms and 33 ms treatments were significantly

Table 2. Comparisons between each treatment and control on a dominant normal distribution with Dunnett-corrected 95% confidence intervals

Variable	0 ms–Control	33 ms–Control	83 ms–Control
Escape trajectory (deg)	**−37.67** to **−5.80**	**−38.46** to **−2.51**	−22.20 to 11.33
Stage 1 turning angle (deg)	**−23.00** to **−5.79**	**−27.15** to **−7.74**	−16.00 to 2.11
Stage 1 turning duration (ms)	**−12.01** to **−1.84**	**−13.07** to **−1.28**	−10.61 to 0.80
Stage 1 turning rate (deg s^{-1})	**−665.34** to **−27.70**	**−746.95** to **−49.18**	−529.92 to 127.86
Stage 2 turning angle (deg)	−5.41 to 12.07	−10.54 to 9.33	−10.16 to 9.15
Stage 2 turning duration (ms)	−10.92 to 4.98	−11.11 to 6.94	−10.45 to 7.11
Stage 2 turning rate (deg s^{-1})	−261.86 to 63.48	**−726.62** to **−364.25**	**−668.82** to **−328.60**
Apparent looming threshold (rad s^{-1})	−2.79 to 1.98	**0.23** to **5.73**	−1.38 to 3.57
Maximum acceleration (cm s^{-2})	−1554.68 to 1667.15	−2156.13 to 1369.53	−1683.05 to 1640.58
Maximum speed (cm s^{-1})	−29.51 to 17.47	−35.59 to 15.83	−27.17 to 21.30
Cumulative distance (cm)	**−2.31** to **−0.71**	−0.70 to 1.12	**−2.37** to **−0.63**

Data are 95% confidence intervals of a dominant normal distribution. Bold indicates a significant difference between the treatment and the control.

smaller than those of the control, while those of the 83 ms treatment were not significantly different from those of the control (Table S1; Fig. 3A,B). The stage 2 turning rate of the 33 ms and 83 ms treatments was significantly lower than that of the control, while that of the 0 ms treatment was not significantly different from that of the control (Table S1). The apparent looming threshold of the 33 ms treatment was significantly higher than that of the control. In contrast, the threshold of the 0 ms and 83 ms treatments was not significantly different from that of the control (Table S1). The cumulative distance of the 0 ms and 83 ms treatments was significantly shorter than that of the control (Table S1). The best model of stage 2 turning rate in the I-T approach was 0 ms≠33 ms=83 ms, indicating that the stage 2 turning rate of the 0 ms treatment was lower than that of the 33 ms and 83 treatments. The best model of the apparent looming threshold was 33 ms≠0 ms=83 ms, indicating that value for the 33 ms treatment was lower than those for the 0 ms and 83 ms treatments. The best models of the other variables were 0 ms=33 ms =83 ms, suggesting no differences in the treatments.

DISCUSSION

The escape trajectories of the staghorn sculpin differed between single and dual threat stimuli when visual stimuli were applied from the left and right sides within 33 ms of one another. The mean of the escape trajectories for a single threat stimulus in the control was 110.60 deg (i.e. escaping away from a single threat stimulus). In contrast, the escape trajectories for dual threat stimuli in the 0 and 33 ms treatments were nearly 90 deg (i.e. perpendicular to the line of attack of dual threat stimuli). Hence, when attacked from two sides simultaneously or with a short delay (33 ms) between dual threat stimuli, fish tended to escape along a 'compromise' trajectory at a similar angle from both stimuli. However, the escape trajectories when the fish were attacked from two sides with a long delay (83 ms) between dual threat stimuli (i.e. when the delayed stimulus occurred after stage 1 initiation) did not differ from those of the single stimulus treatment. Consequently, our findings suggest that the escape trajectory of staghorn sculpin is not fully ballistic and sensory feedback may occur during the initial latency period of the escape responses. Once stage 1 of the escape response is initiated, the escape trajectory is set and is not affected by further feedback control.

Behavioral and neurophysiological studies have shown that the stage 1 turning angles are affected by stimulus direction (Domenici and Blake, 1993; Eaton and Emberley, 1991; Kimura and Kawabata, 2018). Stage 1 turning angles tend to be wide when the stimulus approaches the prey from the front and narrow when the stimulus approaches the prey from behind (Domenici and Blake, 1993; Eaton and Emberley, 1991; Kimura and Kawabata, 2018). The optimal escape trajectory is suggested to range between 90 deg and 180 deg depending on predator speed (Bhattacharyya et al., 2017; Domenici, 2002; Domenici et al., 2011; Weihs and Webb, 1984). Here, the fish were stimulated from the left and right sides. Thus, the resulting escape strategy consisted of remaining at an

Table 3. The results of information-theoretical approach analysis for each variable

Variable	Model	*k*	log*L*	*G*	$V_{gaussian}$	AIC	ΔAIC
Escape trajectories (deg)	0 ms=33 ms=83 ms	4	−221.77	2	E	451.55	0.00
	0 ms=83 ms≠33 ms	9	−217.10	2	E	452.21	0.66
	0 ms=33 ms≠83 ms	9	−217.21	2	E	452.42	0.87
Stage 1 turning angle (deg)	0 ms=33 ms=83 ms	6	−193.67	3	E	399.34	0.00
Stage 1 turning duration (ms)	0 ms=33 ms=83 ms	5	−195.56	2	V	401.13	0.00
Stage 1 turning rate (deg s^{-1})	0 ms=33 ms=83 ms	2	−349.35	1	X	702.69	0.00
Stage 2 turning angle (deg)	0 ms=33 ms=83 ms	2	−135.41	1	X	274.82	0.00
Stage 2 turning duration (ms)	0 ms=33 ms=83 ms	2	−131.08	1	X	266.16	0.00
Stage 2 turning rate (deg s^{-1})	0 ms≠33 ms=83 ms	9	−254.44	2	E	526.88	0.00
	0 ms=33 ms≠83 ms	9	−254.75	2	E	527.50	0.62
Apparent looming threshold (rad s^{-1})	0 ms=83 ms≠33 ms	17	−82.83	3	V	199.66	0.00
Maximum acceleration (cm s^{-2})	0 ms=33 ms=83 ms	2	−427.19	1	X	858.38	0.00
Maximum speed (cm s^{-1})	0 ms=33 ms=83 ms	2	−226.01	1	X	456.01	0.00
Cumulative distance (cm)	0 ms=33 ms=83 ms	5	−84.40	2	V	178.80	0.00

k, number of parameters of the model; log*L*, log likelihood of the model; *G*, number of normal distributions of Gaussian mixture distribution; $V_{gaussian}$, model of variance of Gaussian mixture distribution; X, normal Gaussian distribution; E, Gaussian mixture distributions with equal variance; V, Gaussian mixture distributions with unequal variance; AIC, Akaike's information criterion; ΔAIC, the difference in AIC between each model and the best model. '0 ms', '33 ms' and '83 ms' represent the 0 ms, 33 ms and 83 ms treatment, respectively. '=' indicates that there is no difference between left and right treatments. '≠' indicates there is a difference between left and right treatments. The best model has a ΔAIC value of zero. Each row only shows the results for ΔAIC<2.

equal distance from the two threats by escaping at 90 deg when the two stimuli were simultaneous. The results of the present study suggest that the fish minimize their stage 1 turning angles when they are being attacked from the left and right sides simultaneously. Interestingly, control fish escaped at 110.60 deg (range 74.33–272.35 deg), which appears smaller than the mean escape trajectory (132 deg, range 98–175 deg) of the same species in the previous study (using a single visual stimulus with the same velocity as in this study, but using a nearly square tank) (Paglianti and Domenici, 2006). The rectangular shape of our experimental tank or other unknown factors may have caused this difference.

The mechanism allowing the modulation of stage 1 turning angles in the 0 ms and 33 ms treatments could be related to the activity of M-cells and associated neurons, as well as the prepontine neurons (Marquart et al., 2019). Prepontine neurons facilitate the integration of multiple sensory information (visual and auditory) and alter stage 1 of the escape response (Marquart et al., 2019). It is possible that a similar mechanism may occur in the presence of two visual stimuli, i.e. inputs from the two eyes might be integrated by prepontine neurons before the onset of the escape response. Additionally, the apparent looming threshold of the 33 ms treatment was higher than in the control, which corresponds to an approximately 57 ms delay in the escape latency of the 33 ms treatment. This result suggests that when the fish perceives the second stimulus during neural processing (i.e. between the first stimulation and the onset of stage1), it delays the process based on the single stimulus and integrates the second stimulus information, resulting in a 90 deg escape trajectory from both stimuli. Interestingly, this delay was not observed in the 0 ms treatment, suggesting that two simultaneous stimuli do not cause additional processing, although the mean escape trajectory was also nearly 90 deg (as in the 33 ms treatment), probably as a result of the symmetrical stimuli from both sides.

There were no differences among treatments in terms of their stage 2 turning angles. In stage 2, contraction of the body trunk muscles flips the caudal fin to the opposite side (Foreman and Eaton, 1993). As acceleration increases during stage 2, the body slightly rotates, and the final escape direction is determined. The accelerations and propulsive forces and jets are stronger in stage 2 than they are in stage 1 (Fleuren et al., 2018; Tytell and Lauder, 2008; Voesenek et al., 2019), and they differ in terms of the relative importance of the rotation or acceleration (propulsion) to their movement (Domenici and Blake, 1993; Domenici et al., 2004; Eaton et al., 1977; Eaton and Hackett, 1984; Tytell and Lauder, 2008; Weihs, 1973). Escape trajectories are related to stage 1 turning angles (Domenici and Hale, 2019) and the stage 2 turning angles and rates are smaller than those of stage 1 (Fleuren et al., 2018; Voesenek et al., 2019). Thus, stage 2 plays a relatively more important role in acceleration than it does in escape trajectory. The limited effect of stage 2 on the escape trajectory is in line with the lack of difference in stage 2 turning angles among treatments. Differences between treatments and control were found in cumulative distance, stage 1 turning duration and rate and the stage 2 turning rate. These may be related to the differences of the stage 1 and 2 turning angles.

When the second stimulus reached its threshold after the initiation of the escape response (i.e. in the 83 ms treatment), there was no change in the escape trajectory compared with the control. This is in line with a study on fathead minnows attempting to escape tentacled snakes (Catania, 2009). When fathead minnows were at a strike distance, the tentacled snakes generated a water flow with their bodies and induced a C-start in the fish, directed away from their body but into the snake's mouth. Prey fish cannot modify their escape response after their reaction to the body-generated water flow because one of two M-cells, which fires first, stimulates the body trunk muscle to initiate an escape response but inhibits activation of the opposite body trunk muscle (Faber et al., 1991; Korn and Faber, 2005). In the 83 ms treatment here, it is likely that the M-cell on the stimulus side was activated, with feedback inhibition preventing the activation of the opposing M-cell (Korn and Faber, 2005) as the latter would result in poor escape response performance. As a result, the escape trajectory of the 83 ms treatment did not differ from that of the control. However, our 33 ms treatment suggests that, if stimulated during the neural processing of the first stimulus (i.e. during the escape latency), fish can modify their escape trajectory. Hence, our results demonstrate that fish are capable of receiving additional sensory information during the neurosensory process that involves the circuitry from the optic tectum to the M-cells (Zottoli et al., 1987).

In conclusion, we suggest that the escape response consists of a flexible phase (from stimulation until the onset of stage 1) where sensory feedback is possible, and a ballistic phase (from the onset of stage 1 onwards). The ballistic phase is likely to occur in fish fast escape responses as a result of inhibition of the M-cell to trigger a further contraction during stage 1 (Faber et al., 1991). Specifically, a feed-forward inhibitory network guarantees that when one M-cell is excited, (1) it only generates a single action potential (preventing repetitive firing of one M-cell) and (2) the contralateral M-cell will not be activated. As suggested by Faber et al. (1991), this prevents the occurrence of ineffective escape behaviors, characterized by multiple fast body bends, and bilateral muscle contraction, which would lead to minimal displacement of the fish. While such ineffective motion patterns are prevented, so is the integration of multiple threats within the time interval that corresponds to stage 1. Hence, effective escape is ensured at the cost of eliminating the flexibility that would be associated with sensory feedback during the early phase of the escape response.

We found that Pacific staghorn sculpin can modulate their escape response only between stimulation and the onset of the response, but that escape responses are ballistic after the body motion has started. Although the flexible phase of Pacific staghorn sculpin lasts for at least 33 ms after stimulation, other fish species may show a different relative timing of the flexible and ballistic phases. Identifying which patterns are employed and during which phase may depend on the species and a phylogenetic analysis of escape flexibility would help us understand the evolution of fish escape response patterns. Furthermore, future research integrating behavioral experiments with neurophysiological measures (e.g. calcium imaging) could enable us to understand how the behavioral patterns of the escape response are related to the neural activity when fish are startled by multiple threats.

Acknowledgements
We would like to thank the 2019 Fish Swimming course for support and assistance with fish collections, and Friday Harbor Laboratories, University of Washington, for facilities and technical support. H.K. would like to thank his sponsor, Japan/U.S.–E.S. Morse Scholar Exchange Program and M.L. would like to thank the 'Adopt a Student' program, the Dudley Fund, and the GRIL (Interuniversity Research Group in Limnology and Aquatic Environments) for their financial support to attend the 2019 Fish Swimming course.

Competing interests
The authors declare no competing or financial interests.

Author contributions
Conceptualization: P.D.; Methodology: J.F.S., J.L.J., P.D.; Software: H.K.; Formal analysis: H.K., T.P., M.L., Y.K., P.D.; Investigation: H.K., T.P., M.L.; Resources: H.K.,

T.P., M.L., J.F.S., J.L.J., P.D.; Data curation: H.K., T.P., M.L.; Writing - original draft: H.K.; Writing - review & editing: H.K., T.P., M.L., Y.K., J.L.J., P.D.; Visualization: H.K.; Supervision: Y.K., P.D.; Project administration: P.D.; Funding acquisition: H.K., M.L., Y.K.

Funding

This study was funded by Grants-in-Aid for Scientific Research, Japan Society for the Promotion of Science, to Y.K. (19H04936). H.K. was supported by the Japan/U.S.–E.S. Morse Scholar Exchange Program. M.L. was supported by the University of Washington and by a grant from the GRIL (Groupe de recherche interuniversitaire en limnologie) [a Fonds de Recherche du Québec - Nature et Technologies (FRQNT) funded strategic research network].

Data availability

Data are available from figshare: https://figshare.com/articles/dataset/dataframe_csv/19519033

References

Amo, L., López, P. and Martín, J. (2004). Multiple predators and conflicting refuge use in the wall lizard, *Podarcis muralis*. *Ann. Zool. Fenn.* **41**, 671-679.

Batschelet, E. (1981). *Circular Statistics in Biology*. New York: Academic Press.

Bhattacharyya, K., McLean, D. L. and MacIver, M. A. (2017). Visual threat assessment and reticulospinal encoding of calibrated responses in larval zebrafish. *Curr. Biol.* **27**, 2751-2762.e6. doi:10.1016/j.cub.2017.08.012

Bshary, R., Hohner, A., Ait-el-Djoudi, K. and Fricke, H. (2006). Interspecific communicative and coordinated hunting between groupers and giant moray eels in the Red Sea. *PLoS Biol.* **4**, e431. doi:10.1371/journal.pbio.0040431

Burnham, K. P., Anderson, D. R. and Huyvaert, K. P. (2011). AIC model selection and multimodel inference in behavioral ecology: some background, observations, and comparisons. *Behav. Ecol. Sociobiol.* **65**, 23-35. doi:10.1007/s00265-010-1029-6

Cade, D. E., Carey, N., Domenici, P., Potvin, J. and Goldbogen, J. A. (2020). Predator-informed looming stimulus experiments reveal how large filter feeding whales capture highly maneuverable forage fish. *Proc. Natl. Acad. Sci. USA* **117**, 472-478. doi:10.1073/pnas.1911099116

Catania, K. C. (2009). Tentacled snakes turn C-starts to their advantage and predict future prey behavior. *Proc. Natl. Acad. Sci. USA* **106**, 11183. doi:10.1073/pnas.0905183106

Cooper, W. E., Pérez-Mellado, V. and Hawlena, D. (2007). Number, speeds, and approach paths of predators affect escape behavior by the balearic lizard, *Podarcis lilfordi*. *J. Herpetol.* **41**, 197-204. doi:10.1670/0022-1511(2007)41[197:NSAAPO]2.0.CO;2

Dadda, M., Koolhaas Wouter, H. and Domenici, P. (2010). Behavioural asymmetry affects escape performance in a teleost fish. *Biol. Lett.* **6**, 414-417. doi:10.1098/rsbl.2009.0904

Dayton, C. M. (1998). Information criteria for the paired-comparisons problem. *Am. Stat.* **52**, 144-151. doi:10.1080/00031305.1998.10480554

Dill, L. M. (1974). The escape response of the zebra danio (*Brachydanio rerio*) I. The stimulus for escape. *Anim. Behav.* **22**, 711-722. doi:10.1016/S0003-3472(74)80022-9

Domenici, P. (2002). The visually mediated escape response in fish: predicting prey responsiveness and the locomotor behaviour of predators and prey. *Mar. Freshw. Behav. Physiol.* **35**, 87-110. doi:10.1080/10236240290025635

Domenici, P. and Blake, R. W. (1993). Escape trajectories in angelfish (*Pterophyllum eimekei*). *J. Exp. Biol.* **177**, 253-272. doi:10.1242/jeb.177.1.253

Domenici, P. and Blake, R. (1997). The kinematics and performance of fish fast-start swimming. *J. Exp. Biol.* **200**, 1165-1178. doi:10.1242/jeb.200.8.1165

Domenici, P. and Hale, M. E. (2019). Escape responses of fish: a review of the diversity in motor control, kinematics and behaviour. *J. Exp. Biol.* **222**, jeb166009. doi:10.1242/jeb.166009

Domenici, P. and Ruxton, G. D. (2015). Prey behaviors during fleeing: escape trajectories, signaling and sensory defenses. In *Escaping from Predators: An Integrative View of Escape Decisions* (ed. W. E. Cooper and D. T. Blumstein), pp. 199-224. Cambridge University Press.

Domenici, P., Standen, E. M. and Levine, R. P. (2004). Escape manoeuvres in the spiny dogfish (*Squalus acanthias*). *J. Exp. Biol.* **207**, 2339-2349. doi:10.1242/jeb.01015

Domenici, P., Booth, D., Blagburn, J. M. and Bacon, J. P. (2008). Cockroaches keep predators guessing by using preferred escape trajectories. *Curr. Biol.* **18**, 1792-1796. doi:10.1016/j.cub.2008.09.062

Domenici, P., Blagburn, J. M. and Bacon, J. P. (2011). Animal escapology I: theoretical issues and emerging trends in escape trajectories. *J. Exp. Biol.* **214**, 2463-2473. doi:10.1242/jeb.029652

Dunnett, C. W. (1964). New table for multiple comparisons with a control biometrics. *Biometrics* **20**, 482-491. doi:10.2307/2528490

Eaton, R. C. and Emberley, D. S. (1991). How stimulus direction determines the trajectory of the Mauthner-initiated escape response in a teleost fish. *J. Exp. Biol.* **161**, 469-487. doi:10.1242/jeb.161.1.469

Eaton, R. C. and Hackett, J. T. (1984). The role of the Mauthner cell in fast-starts involving escape in teleost fishes. In *Neural Mechanisms of Startle Behavior* (ed. R. C. Eaton), pp. 213-266. Boston, MA: Springer US.

Eaton, R. C., Bombardieri, R. A. and Meyer, D. L. (1977). The Mauthner-initiated startle response in teleost fish. *J. Exp. Biol.* **66**, 65-81. doi:10.1242/jeb.66.1.65

Eaton, R. C., Lavender, W. A. and Wieland, C. M. (1981). Identification of Mauthner-initiated response patterns in goldfish: evidence from simultaneous cinematography and electrophysiology. *J. Comp. Physiol. A* **144**, 521-531. doi:10.1007/BF01326837

Eaton, R. C., DiDomenico, R. and Nissanov, J. (1988). Flexible body dynamics of the goldfish C-start: implications for reticulospinal command mechanisms. *J. Neurosci.* **8**, 2758. doi:10.1523/JNEUROSCI.08-08-02758.1988

Eaton, R. C., Lee, R. K. K. and Foreman, M. B. (2001). The Mauthner cell and other identified neurons of the brainstem escape network of fish. *Prog. Neurobiol.* **63**, 467-485. doi:10.1016/S0301-0082(00)00047-2

Faber, D. S., Korn, H. and Lin, J.-W. (1991). Role of medullary networks and postsynaptic membrane properties in regulating Mauthner cell responsiveness to sensory excitation. *Brain Behav. Evol.* **37**, 286-297. doi:10.1159/000114366

Fleuren, M., van Leeuwen, J. L., Quicazan-Rubio, E. M., Pieters, R. P. M., Pollux, B. J. A. and Voesenek, C. J. (2018). Three-dimensional analysis of the fast-start escape response of the least killifish, *Heterandria formosa*. *J. Exp. Biol.* **221**, jeb168609. doi:10.1242/jeb.168609

Foreman, M. B. and Eaton, R. C. (1993). The direction change concept for reticulospinal control of goldfish escape. *J. Neurosci.* **13**, 4101. doi:10.1523/JNEUROSCI.13-10-04101.1993

Halsey, L. G. (2019). The reign of the p-value is over: what alternative analyses could we employ to fill the power vacuum? *Biol. Lett.* **15**, 20190174. doi:10.1098/rsbl.2019.0174

Hecker, A., Schulze, W., Oster, J., Richter, D. O. and Schuster, S. (2020). Removing a single neuron in a vertebrate brain forever abolishes an essential behavior. *Proc. Natl. Acad. Sci. USA* **117**, 3254-3260. doi:10.1073/pnas.1918578117

Hein, A. M., Gil, M. A., Twomey, C. R., Couzin, I. D. and Levin, S. A. (2018). Conserved behavioral circuits govern high-speed decision-making in wild fish shoals. *Proc. Natl. Acad. Sci. USA* **115**, 12224-12228. doi:10.1073/pnas.1809140115

Kimura, H. and Kawabata, Y. (2018). Effect of initial body orientation on escape probability of prey fish escaping from predators. *Biol. Open* **7**, bio023812. doi:10.1242/bio.023812

Korn, H. and Faber, D. S. (2005). The Mauthner cell half a century later: a neurobiological model for decision-making? *Neuron* **47**, 13-28. doi:10.1016/j.neuron.2005.05.019

Lanczos, C. (1956). *Applied Analysis*. Englewood Cliffs, NJ: Prentice-Hall.

Marquart, G. D., Tabor, K. M., Bergeron, S. A., Briggman, K. L. and Burgess, H. A. (2019). Prepontine non-giant neurons drive flexible escape behavior in zebrafish. *PLoS Biol.* **17**, e3000480. doi:10.1371/journal.pbio.3000480

Mirjany, M. and Faber, D. S. (2011). Characteristics of the anterior lateral line nerve input to the Mauthner cell. *J. Exp. Biol.* **214**, 3368-3377. doi:10.1242/jeb.056226

Paglianti, A. and Domenici, P. (2006). The effect of size on the timing of visually mediated escape behaviour in staghorn sculpin *Leptocottus armatus*. *J. Fish Biol.* **68**, 1177-1191. doi:10.1111/j.0022-1112.2006.00991.x

Richards, S. A., Whittingham, M. J. and Stephens, P. A. (2011). Model selection and model averaging in behavioural ecology: the utility of the IT-AIC framework. *Behav. Ecol. Sociobiol.* **65**, 77-89. doi:10.1007/s00265-010-1035-8

Russell, I. J. (1976). Central inhibition of lateral line input in the medulla of the goldfish by neurones which control active body movements. *J. Comp. Physiol. A* **111**, 335-358. doi:10.1007/BF00606471

Sato, N., Shidara, H. and Ogawa, H. (2019). Trade-off between motor performance and behavioural flexibility in the action selection of cricket escape behaviour. *Sci. Rep.* **9**, 18112. doi:10.1038/s41598-019-54555-7

Scrucca, L., Fop, M., Murphy, T. B. and Raftery, A. E. (2016). mclust 5: clustering, classification and density estimation using Gaussian finite mixture models. *R J.* **8**, 289-317. doi:10.32614/RJ-2016-021

Stander, P. E. (1992). Cooperative hunting in lions: the role of the individual. *Behav. Ecol. Sociobiol.* **29**, 445-454. doi:10.1007/BF00170175

Steinegger, M., Roche, D. G. and Bshary, R. (2018). Simple decision rules underlie collaborative hunting in yellow saddle goatfish. *Proc. R. Soc. B Biol. Sci.* **285**, 20172488. doi:10.1098/rspb.2017.2488

Stewart, W. J., Cardenas, G. S. and McHenry, M. J. (2013). Zebrafish larvae evade predators by sensing water flow. *J. Exp. Biol.* **216**, 388-398. doi:10.1242/jeb.072751

Stewart, W. J., Nair, A., Jiang, H. and McHenry, M. J. (2014). Prey fish escape by sensing the bow wave of a predator. *J. Exp. Biol.* **217**, 4328-4336. doi:10.1242/jeb.111773

Sugiura, N. (1978). Further analysts of the data by akaike' s information criterion and the finite corrections. *Commun. Stat. Theory Methods* **7**, 13-26. doi:10.1080/03610927808827599

Temizer, I., Donovan, J. C., Baier, H. and Semmelhack, J. L. (2015). A visual pathway for looming-evoked escape in larval zebrafish. *Curr. Biol.* **25**, 1823-1834. doi:10.1016/j.cub.2015.06.002

Tytell, E. D. and Lauder, G. V. (2008). Hydrodynamics of the escape response in bluegill sunfish, *Lepomis macrochirus*. *J. Exp. Biol.* **211**, 3359-3369. doi:10.1242/jeb.020917

Voesenek, C. J., Pieters, R. P. M., Muijres, F. T. and van Leeuwen, J. L. (2019). Reorientation and propulsion in fast-starting zebrafish larvae: an inverse dynamics analysis. *J. Exp. Biol.* **222**, jeb203091. doi:10.1242/jeb.203091

Walker, J. A., Ghalambor, C. K., Griset, O. L., McKenney, D. and Reznick, D. N. (2005). Do faster starts increase the probability of evading predators? *Funct. Ecol.* **19**, 808-815. doi:10.1111/j.1365-2435.2005.01033.x

Weihs, D. (1973). The mechanism of rapid starting of slender fish[1]. *Biorheology* **10**, 343-350. doi:10.3233/BIR-1973-10308

Weihs, D. and Webb, P. W. (1984). Optimal avoidance and evasion tactics in predator-prey interactions. *J. Theor. Biol.* **106**, 189-206. doi:10.1016/0022-5193(84)90019-5

Zottoli, S. J., Marek, L. E., Agostini, M. A. and Strittmatter, S. L. (1987). Morphological and physiological survival of goldfish Mauthner axons isolated from their somata by spinal cord crush. *J. Comp. Neurol.* **255**, 272-282. doi:10.1002/cne.902550210